Supplementary Information for Distributional Impacts of 1.5 °C Overshoot Pathways: Food, Energy, and the Limits of Carbon Revenue Recycling

Jiarui Zhong[1,*], Franziska Piontek[1], Benjamin Leon Bodirsky[1], David Meng-Chuen Chen[1,2,3], Leonard Missbach[1], Robin Hasse[1,4], Leon Merfort[1,4], Tabea Dorndorf[1,5], Anne Merfort[1,4], Benjamin Peeters[1], Johannes Koch[1], Elmar Kriegler[1,6]

[1]Potsdam Institute for Climate Impact Research
[2]Humboldt-Universität zu Berlin (HU), Albrecht Daniel Thaer-Institut für Agrar- und Gartenbauwissenschaften, Germany
[3]Humboldt-Universität zu Berlin, Integrative Research Institute on Transformations of Human-Environment Systems (IRI THESys), Berlin, Germany
[4]Global Energy Systems Analysis, Technische Universität Berlin, Berlin, Germany
[5]Humboldt-Universität zu Berlin, Geographic Institute, Germany
[6]University of Potsdam
*Corresponding author: jiarui.zhong@pik-potsdam.com

Contents

S1 Summary of integrated assessment framework and scenario design

Figure S1 provides an overview of the modelling framework used in this study and the flow of information between its main components. It illustrates how scenario outputs from REMIND–MAgPIE are linked to the distributional module to derive household-level welfare and inequality outcomes.

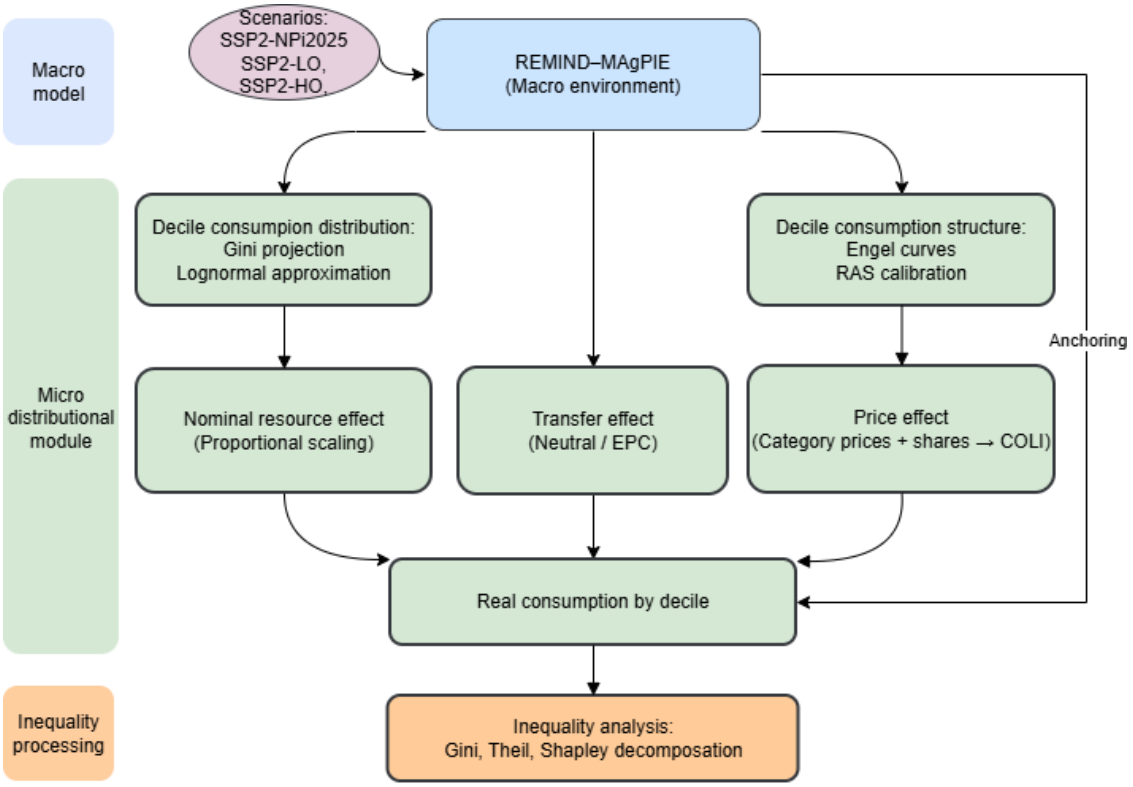

Supplementary Figure S1: Overview of the modelling framework and information flow across modules.

S2 Within-region expenditure inequality in baseline and policy scenarios

S2.1 Constructing regional decile shares from country income Gini index

For the within-region distribution of consumption expenditure in monetary terms, we assume that expenditure in both the baseline and policy scenarios follows the exogenous SSP2 inequality projections. This implies that, when regional consumption is downscaled to within-region deciles, all

three scenarios share the same within-region inequality, and mitigation-induced changes in nominal consumption are distribution-neutral within each period. Across periods, however, the distribution evolves according to the projected dynamics of the Gini coefficient.

We use the inequality projections from [1], which were developed for the first generation of quantitative SSP implementations [2]. By contrast, the REMIND–MAgPIE scenarios used in this study are calibrated to the most recent release of the SSP public database [3], which incorporates updated projections of population, education, and macroeconomic development. We therefore combine inequality trajectories derived under the first-generation SSP quantification with macroeconomic projections based on the updated SSP database. This approach can be revised once updated inequality projections consistent with the latest SSP database become available.

While the underlying SSP narratives remain unchanged, successive database releases introduce revisions to demographic and economic trajectories. The use of the earlier inequality projections reflects current data availability; once updated SSP-consistent inequality projections become available, they can be incorporated directly within the same modelling framework.

This section documents two technical steps used to map country-level inequality information to the regional decile structure required by our consumption module.

S2.1.1 Aggregating country Gini to regional Gini

This section documents the procedure used to aggregate country-level Gini coefficients to the regional level. Because the Gini index is not additively decomposable, direct aggregation is not feasible. We therefore proceed by mapping country-level Gini coefficients to a decomposable inequality measure under a parametric distributional assumption [4].

Lognormal assumption. We assume that the consumption expenditure in each country c follows a lognormal distribution,

$$Y_c \sim \text{LogNormal}(\mu_c, \sigma_c^2).$$

Under the lognormal distribution, the Gini coefficient is a one-to-one function of the log-variance parameter σ_c:

$$G_c = 2\,\Phi\left(\frac{\sigma_c}{\sqrt{2}}\right) - 1,$$

where $\Phi(\cdot)$ denotes the standard normal cumulative distribution function. Solving for σ_c yields

$$\sigma_c = \sqrt{2}\,\Phi^{-1}\left(\frac{G_c + 1}{2}\right).$$

This allows us to recover the implied dispersion parameter for each country based solely on its Gini coefficient.

Conversion to Theil index. Under the lognormal distribution, the generalized entropy indices Theil-T and Theil-L coincide and are given by

$$T_c = L_c = \frac{1}{2}\sigma_c^2,$$

which provides a consistent mapping from the observed Gini coefficient to a decomposable inequality measure.

Regional aggregation via Theil decomposition. Let region r consist of countries $c \in r$. Denote by p_c the population share of country c in region r, by μ_c the mean consumption of country c, and by μ_r the regional mean consumption. Define consumption weights

$$s_c = \frac{p_c \mu_c}{\sum_{j \in r} p_j \mu_j}.$$

The Theil index is additively decomposable; using Theil-T for a region r it can be written compactly as

$$T_r = \sum_{c \in r} s_c \, T_c + \sum_{c \in r} s_c \, \ln\!\left(\frac{\mu_c}{\mu_r}\right).$$

Back-transformation to regional Gini. Finally, we convert the aggregated regional Theil index T_r back to a Gini coefficient using the lognormal mapping:

$$G_r = 2\,\Phi\!\left(\sqrt{T_r}\right) - 1.$$

Interpretation and limitations. This procedure yields a regionally consistent inequality measure that (i) preserves additivity through the Theil index, (ii) incorporates both within-country and between-country inequality, and (iii) remains internally consistent under the lognormal distributional assumption. The lognormal assumption is a pragmatic choice given data availability: because only country-level Gini coefficients are observed, higher moments of the consumption distribution cannot be identified. Alternative parametric distributions (e.g., GB2 or generalized gamma) could be employed if additional distributional information were available.

S2.1.2 From regional Gini to regional decile consumption shares

Second, we translate the regional Gini $G_{r,t}$ into decile mean consumption levels and corresponding decile shares. We take the IAM representative-household consumption expenditure for each region and year, denoted $E_{r,t}$, as the regional mean of total nominal resources.

Distributional representation. Consistent with the lognormal assumption introduced above, let $y_{r,t}$ denote per-capita consumption in region r at time t and assume

$$\ln y_{r,t} \sim \mathcal{N}(\mu_{r,t}, \sigma_{r,t}^2).$$

The parameters $(\mu_{r,t}, \sigma_{r,t})$ are pinned down by the IAM mean consumption $E_{r,t}$ and the regional Gini coefficient $G_{r,t}$ using the same lognormal mapping as in Section S2.2.1. Given $(\mu_{r,t}, \sigma_{r,t})$, the regional consumption distribution is fully identified.

Decile means and shares. Let q_h denote the decile cutoffs with $q_0 = 0$, $q_1 = 0.1$, ..., $q_{10} = 1$. Average per-capita consumption in decile $h \in \{1, \ldots, 10\}$ is computed as the conditional mean over the corresponding quantile interval,

$$\bar{y}_{r,h,t} = \frac{1}{q_h - q_{h-1}} \int_{q_{h-1}}^{q_h} \exp\big(\mu_{r,t} + \sigma_{r,t}\, \Phi^{-1}(u)\big)\, du.$$

We then define decile consumption shares as

$$s_{r,h,t} = \frac{\bar{y}_{r,h,t}}{\sum_{h=1}^{10} \bar{y}_{r,h,t}},$$

which by construction sum to one.

Consistency between income and consumption inequality. Income Ginis are typically higher than consumption Ginis because households smooth consumption and engage in saving behavior [5, 6]. The inequality projections in Rao et al. [1] draw on global datasets that combine income- and expenditure-based Gini coefficients. We therefore interpret the SSP-projected income Gini trajectories as reflecting the overall distribution of household consumption and use them to downscale aggregate regional consumption across deciles.

The regional expenditure distributions for selected years are shown in Fig. S2.

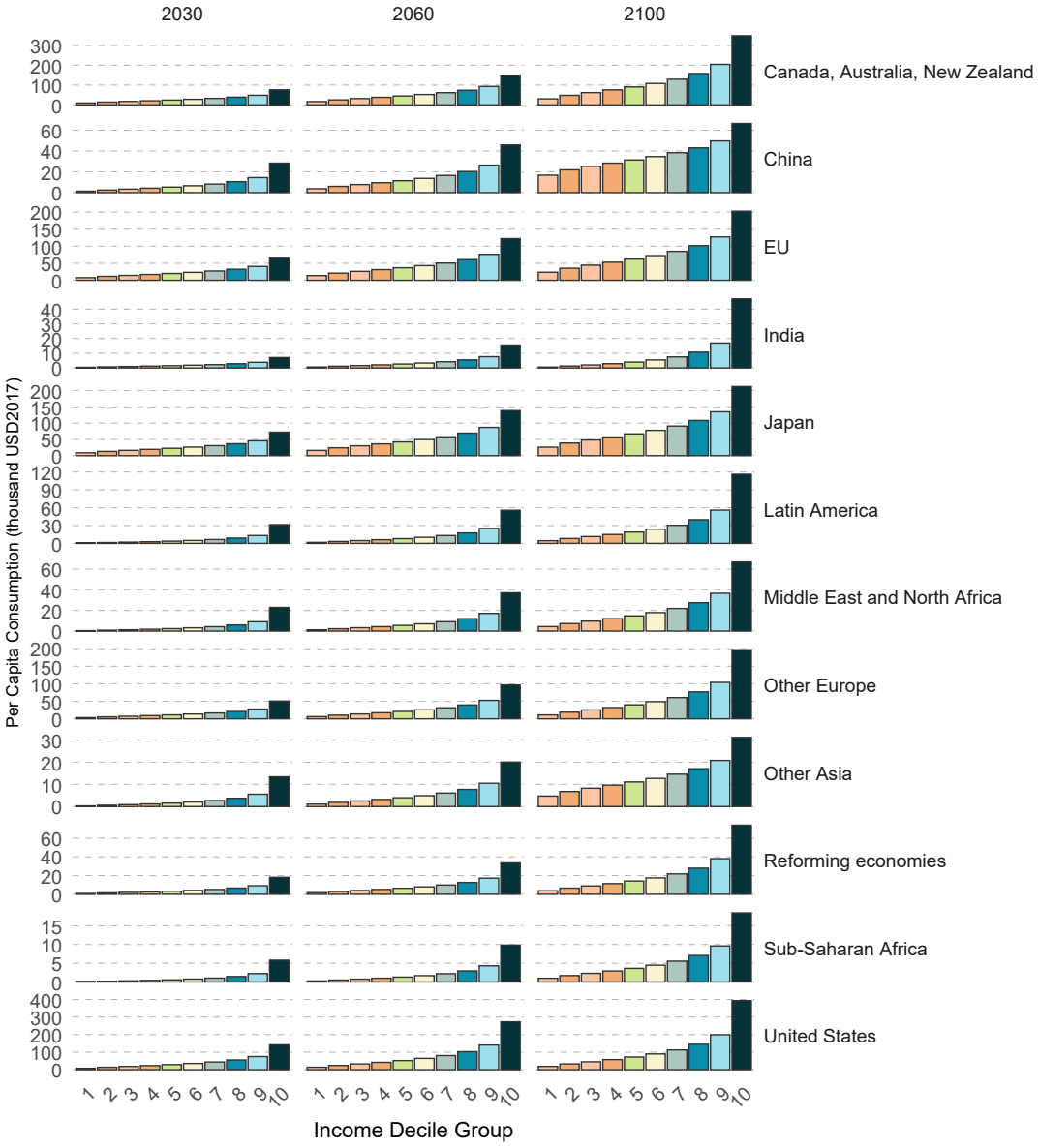

Supplementary Figure S2: Mapping regional inequality to decile consumption shares. Illustration of the lognormal calibration using the regional mean consumption $E_{r,t}$ and Gini coefficient $G_{r,t}$, and the resulting implied decile mean consumption levels and consumption shares.

S3 Empirical Estimation of Engel Curves

S3.1 Data construction and cleaning for Engel curve estimation

The estimation of Engel curves is based on the global consumption dataset [7]. We aggregate the national micro data to 10 consumption deciles for each country, so that the unit of observation is a country–decile cell. We further harmonize MCC expenditure items by mapping them to the nine consumption categories used in REMIND–MAgPIE. The observed variables are categorical expenditure shares and expenditure.

Each country–decile cell contains:

- Total household consumption expenditure (in 2017 USD)
- Expenditure shares for nine consumption categories, namely:
  - Animal products
  - Staples
  - Fruits vegetables nuts
  - Processed food
  - Building electricity
  - Building gases
  - Building other fuels
  - Transport energy
  - Other commodities

In the MCC dataset, category shares are computed as category-specific expenditure divided by total household consumption expenditure reported in the survey. Due to potential under-reporting, misreporting, or other measurement errors, the nine category shares do not always sum to one exactly. To ensure internal consistency of the consumption baskets used for estimation, we apply a share-closure check and retain only observations that satisfy

$$\sum_{g} w_{c,h,g} \in [0.9, 1.1],$$

where c indexes countries, h indexes consumption deciles, and g indexes consumption categories. This tolerance band allows for moderate measurement error while excluding observations with clearly incomplete or structurally inconsistent consumption baskets. The filtered sample is used for subsequent Engel curve estimation.

S3.2 Econometric specification of Engel curves

S3.2.1 Regression model

For each consumption category g, Engel curves are estimated separately using the following specification:

$$\text{logit}(w_{r,c,h,g}) = \alpha_{r,g} + \beta_{r,g,1} \ln E_{r,c,h} + \beta_{r,g,2} (\ln E_{r,c,h})^2 + \delta_{r,c} + \varepsilon_{r,c,h,g}.$$

where:

- $w_{r,c,h,g}$ denotes the expenditure share;
- $E_{r,c,h}$ denotes total expenditure of decile h;
- $\delta_{r,c}$ denotes country fixed effects.

To avoid numerical instability in the logit transformation near 0 or 1, shares are clipped to the interval $[10^{-6}, 1 - 10^{-6}]$ prior to transformation.

Estimation is conducted using weighted least squares (WLS), with decile population weights applied at the country–decile level.

S3.2.2 Regional and pooled estimation

While Engel curves theoretically capture consumption patterns across different expenditure levels and stages of economic development, they are also shaped by regional cultural backgrounds and other local characteristics. Estimating only a global Engel curve would therefore miss important regional differences in consumption behavior. We therefore estimate both regional and pooled Engel curves and assess whether regional heterogeneity needs to be taken into account.

Regional Engel curves. Countries are grouped according to the REMIND-MAgPIE H12 regional classification, and estimation is performed separately for each region. Within each region, countries are pooled and country fixed effects are included whenever at least two countries are available. This specification allows the slope parameters $\beta_{r,g,1}$ and $\beta_{r,g,2}$ to vary across regions, thereby capturing regional heterogeneity in consumption structure.

A comparison of the regional Engel curves in Fig. S3 shows substantial heterogeneity across regions, which justifies using regional rather than a uniform global Engel curve. However, their historical support ranges (solid lines) are relatively limited, so relying exclusively on them would increase the risk of over-extrapolation and lead to unreliable estimates.

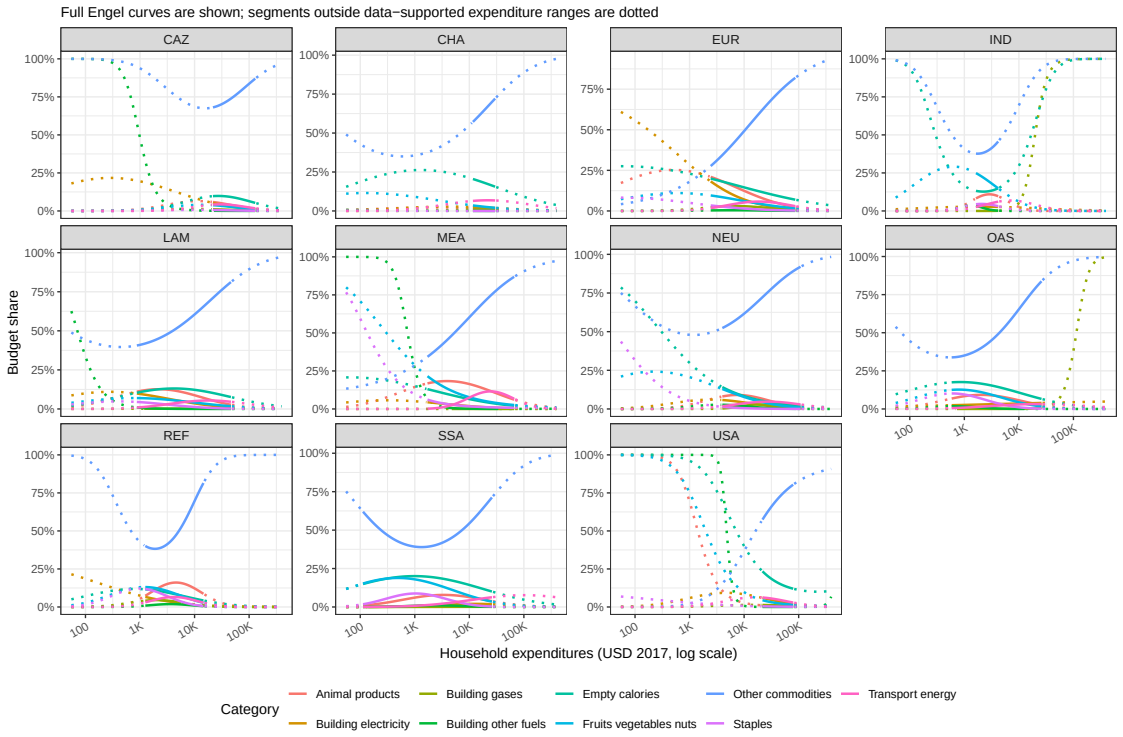

Supplementary Figure S3: Regional Engel curves estimated with data-supported ranges.

We show selected regional regression results below.

Supplementary Table S1: Regional Engel curve estimates for EUR

Statistic	Animal products	Building electricity	Empty calories	Transport energy	Fruits vegetables nuts	Building gases	Building other fuels	Other commodities	Staples
Intercept	-4.934***	1.225	-1.023	-31.283***	-5.714***	-24.598***	-24.959***	-5.093***	-3.043**
Intercept SE	(1.583)	(1.632)	(1.948)	(1.773)	(1.429)	(2.455)	(5.275)	(1.902)	(1.500)
log(exp)	1.226***	0.049	0.251	5.790***	1.044***	4.782***	4.836***	0.379	0.573*
log(exp) SE	(0.320)	(0.330)	(0.394)	(0.359)	(0.289)	(0.497)	(1.067)	(0.385)	(0.304)
$I(\log(\exp)^2)$	-0.098***	-0.048***	-0.031	-0.295***	-0.082***	-0.270***	-0.279***	0.016	-0.069***
$I(\log(\exp)^2)$ SE	(0.016)	(0.017)	(0.020)	(0.018)	(0.015)	(0.025)	(0.054)	(0.019)	(0.015)
R^2	0.951	0.942	0.938	0.870	0.945	0.979	0.943	0.917	0.981
Adjusted R^2	0.945	0.935	0.930	0.854	0.939	0.977	0.937	0.907	0.979
Observations	250	260	260	260	250	260	260	260	250
Country FE	Yes	Yes	Yes	Yes	Yes	Yes	Yes	Yes	Yes

Notes: * $p < 0.1$; ** $p < 0.05$; *** $p < 0.01$.

Supplementary Table S2: Regional Engel curve estimates for USA

Statistic	Animal products	Building electricity	Empty calories	Transport energy	Fruits vegetables nuts	Building gases	Building other fuels	Other commodities	Staples
Intercept	28.360***	-16.955	25.788***	-33.495***	18.446**	-25.633	182.072	-20.517***	-9.210***
Intercept SE	(3.998)	(13.832)	(5.981)	(5.468)	(5.581)	(17.455)	(188.484)	(3.763)	(0.000)
log(exp)	-5.544***	3.470	-4.540***	6.354***	-3.306**	4.449	-35.226	3.169***	0.000
log(exp) SE	(0.753)	(2.605)	(1.126)	(1.030)	(1.051)	(3.287)	(35.494)	(0.709)	(0.000)
$I(\log(\exp)^2)$	0.225***	-0.205	0.184**	-0.328***	0.115*	-0.232	1.621	-0.109**	-0.000
$I(\log(\exp)^2)$ SE	(0.035)	(0.123)	(0.053)	(0.048)	(0.049)	(0.155)	(1.670)	(0.033)	(0.000)
R^2	0.997	0.973	0.990	0.991	0.995	0.869	0.217	0.998	0.461
Adjusted R^2	0.996	0.965	0.987	0.989	0.994	0.832	-0.007	0.997	0.308
Observations	10	10	10	10	10	10	10	10	10
Country FE	No	No	No	No	No	No	No	No	No

Notes: * $p < 0.1$; ** $p < 0.05$; *** $p < 0.01$.

Supplementary Table S3: Regional Engel curve estimates for REF

Statistic	Animal products	Building electricity	Empty calories	Transport energy	Fruits vegetables nuts	Building gases	Building other fuels	Other commodities	Staples
Intercept	-38.735***	-0.997	-7.826*	-41.255***	-15.423***	-26.025***	-47.737***	26.126***	-21.702***
Intercept SE	(3.493)	(1.945)	(4.131)	(1.892)	(1.962)	(4.005)	(10.464)	(3.133)	(1.224)
log(exp)	8.799***	0.128	1.742	9.264***	3.813***	6.039***	10.683***	-7.059***	5.736***
log(exp) SE	(0.887)	(0.494)	(1.049)	(0.480)	(0.498)	(1.017)	(2.656)	(0.795)	(0.311)
$I(\log(\exp)^2)$	-0.522***	-0.050	-0.130*	-0.556***	-0.269***	-0.397***	-0.652***	0.468***	-0.417***
$I(\log(\exp)^2)$ SE	(0.056)	(0.031)	(0.066)	(0.030)	(0.032)	(0.064)	(0.168)	(0.050)	(0.020)
R^2	0.965	0.996	0.835	0.987	0.978	0.918	0.689	0.936	0.998
Adjusted R^2	0.958	0.994	0.804	0.985	0.974	0.895	0.631	0.924	0.997
Observations	20	10	20	20	20	10	20	20	20
Country FE	Yes	No	Yes	Yes	Yes	No	Yes	Yes	Yes

Notes: * $p < 0.1$; ** $p < 0.05$; *** $p < 0.01$.

Supplementary Table S4: Regional Engel curve estimates for SSA

Statistic	Animal products	Building electricity	Empty calories	Transport energy	Fruits vegetables nuts	Building gases	Building other fuels	Other commodities	Staples
Intercept	-15.247***	-24.776***	-5.223***	-16.348***	-6.558***	-23.102***	-27.964***	8.181***	-18.805***
Intercept SE	(0.952)	(1.748)	(0.697)	(1.799)	(0.547)	(5.149)	(2.131)	(0.597)	(1.031)
log(exp)	2.989***	4.396***	1.045***	2.579***	1.463***	3.273**	6.173***	-2.210***	4.681***
log(exp) SE	(0.250)	(0.459)	(0.183)	(0.464)	(0.144)	(1.279)	(0.559)	(0.157)	(0.271)
$I(\log(\exp)^2)$	-0.184***	-0.232***	-0.076***	-0.112***	-0.118***	-0.168**	-0.396***	0.154***	-0.337***
$I(\log(\exp)^2)$ SE	(0.017)	(0.031)	(0.012)	(0.030)	(0.010)	(0.080)	(0.037)	(0.010)	(0.018)
R^2	0.835	0.900	0.806	0.893	0.966	0.540	0.842	0.910	0.881
Adjusted R^2	0.815	0.888	0.783	0.880	0.962	0.483	0.824	0.900	0.867
Observations	180	180	180	170	180	110	180	180	180
Country FE	Yes	Yes	Yes	Yes	Yes	Yes	Yes	Yes	Yes

Notes: * $p < 0.1$; ** $p < 0.05$; *** $p < 0.01$.

Pooled (global) Engel curves. While pooled Engel curves do not capture regional characteristics, they are more robust because they are estimated from more observations and span a wider consumption expenditure range. They therefore provide an Engel curve with broader empirical support. To estimate the pooled global Engel curve, all countries are combined into a single regression that retains country fixed effects while imposing common slope parameters across regions. Under this specification, all regions share the same Engel curve shape (S4).

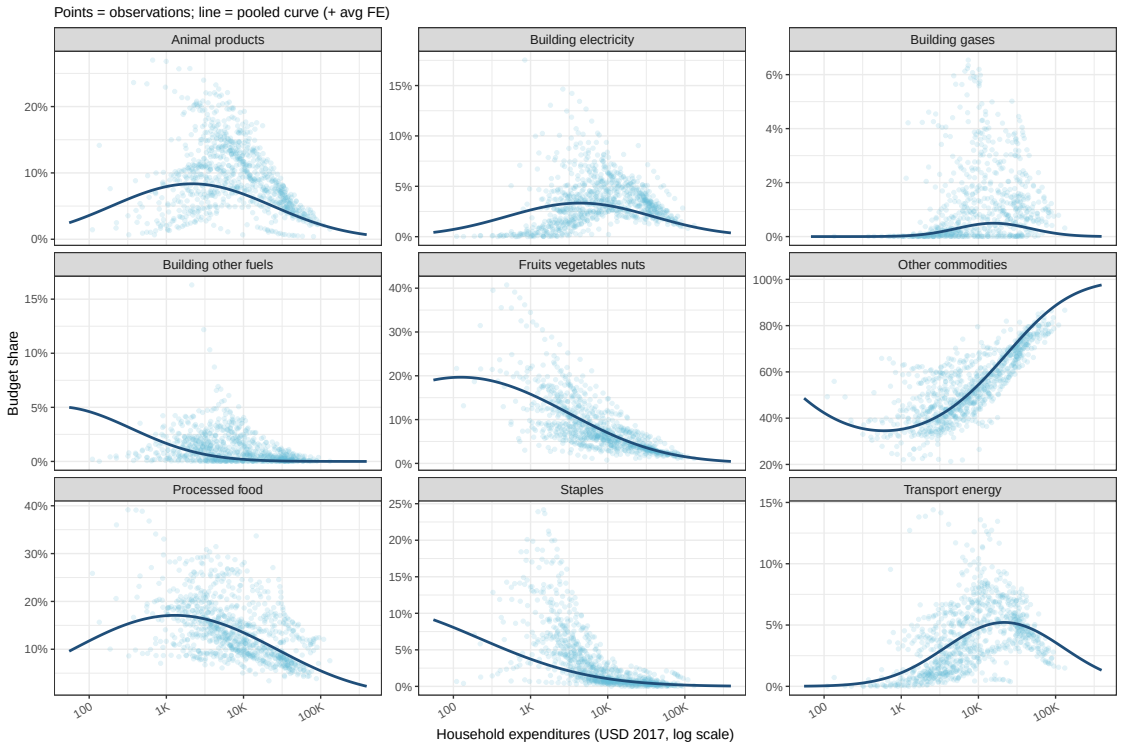

Supplementary Figure S4: Pooled (global) Engel curves and data points.

Supplementary Table S5: Pooled unconstrained Engel curve estimates for MCC sectors

Statistic	Animal products	Building electricity	Empty calories	Transport energy	Fruits, vegetables, nuts	Building gases	Building other fuels	Other commodities	Staples
Intercept	-11.968***	-20.255***	-4.816***	-21.369***	-3.493***	-41.902***	-3.550**	3.192***	-4.056***
Intercept SE	(0.433)	(0.610)	(0.322)	(0.790)	(0.304)	(2.407)	(1.558)	(0.275)	(0.555)
log(exp)	2.702***	4.299***	0.957***	3.797***	0.702***	7.987***	0.782**	-1.313***	0.544***
log(exp) SE	(0.099)	(0.140)	(0.074)	(0.180)	(0.070)	(0.534)	(0.374)	(0.063)	(0.127)
$I(\log(\text{exp})^2)$	-0.171***	-0.260***	-0.067***	-0.195***	-0.068***	-0.413***	-0.107***	0.103***	-0.068***
$I(\log(\text{exp})^2)$ SE	(0.006)	(0.008)	(0.004)	(0.010)	(0.004)	(0.030)	(0.022)	(0.004)	(0.007)
R^2	0.968	0.900	0.908	0.914	0.982	0.919	0.891	0.967	0.988
Adjusted R^2	0.965	0.888	0.898	0.904	0.980	0.909	0.879	0.963	0.987
Observations	856	856	866	856	856	657	776	866	856
Country FE	Yes	Yes	Yes	Yes	Yes	Yes	Yes	Yes	Yes

Notes: * $p < 0.1$; ** $p < 0.05$; *** $p < 0.01$.

Note that this table reports the results from the unconstrained regression. For the projection analysis, we use the results from the constrained regression (see Section S4.1).

S3.2.3 Regional heterogeneity and robustness

Estimation results indicate substantial cross-regional differences in slope parameters for several consumption categories, particularly for food and energy goods. Regional Engel curves capture these differences, but their empirically supported ranges are relatively narrow. By contrast, the pooled specification imposes homogeneous slope parameters across regions and may therefore attenuate region-specific structural differences, but it is more robust for projections in which deciles become

substantially richer. To balance heterogeneity against robustness, we use regional Engel curves wherever possible, that is, when the relevant coefficients can be estimated and the projection remains reasonably close to the historical support. Otherwise, the projection falls back to the global Engel curve.

S3.2.4 Parameter overrides and local corrections

While regional estimates are preferred, there are two regions for which the estimates are either unavailable or not representative: JPN and CHA. For Japan, the dataset contains no usable observations, so no regional estimates can be obtained. In this case, we fall back to the pooled estimates.

For CHA, the dataset contains observations only for Hong Kong. Because Hong Kong represents a much smaller population than mainland China and has a substantially higher expenditure level, the resulting regional estimates are not considered representative of the broader region. We therefore also use the pooled Engel curve for projections in CHA.

For the Staples category in the USA, the consumption dataset reports no consumption data across all deciles. As a result, the regional Engel curve cannot identify the expenditure response for this category. Therefore, pooled Engel curve parameters are used for this specific region–category combination.

S4 Projection of Decile Categorical Shares

S4.1 Engel curve projection: regional projection and out-of-sample extrapolation

Projection based on regional Engel curves For region r, category g, decile h, and year t, the regional consumption share is obtained by evaluating the regional Engel curve at projected expenditure levels:

$$s^{\text{Reg}}_{r,g,h,t} = \text{logit}^{-1}\big(\alpha_{r,g} + \beta_{r,g,1} \ln E_{r,h,t} + \beta_{r,g,2} (\ln E_{r,h,t})^2\big) .$$

Within the range of observed data, these projections preserve region-specific consumption structures and reproduce the empirically observed heterogeneity across expenditure groups.

When projecting to future periods, however, expenditure levels—especially for upper deciles—can substantially exceed the range observed in household survey data. Applying regional Engel curves

outside their empirical support can therefore lead to unstable extrapolation, because polynomial Engel curves often behave erratically in the tails. This motivates the structured extrapolation approach described below.

Two-stage Engel curve extrapolation To ensure robust projections beyond the observed data range, we implement a two-stage extrapolation procedure that retains regional Engel curves where the data are informative and transitions to more robust pooled behavior in the tails.

Let $s^{\text{Reg}}_{r,g,h,t}$ denote the share from the regional Engel curve and $s^{\text{Glob}}_{r,g,h,t}$ the share from the pooled (global) Engel curve.

Stage 1: Region–year blending Stage 1 implements the transition from regional to pooled Engel curves once projected expenditure levels move beyond regional empirical support. Let $x_{r,h,t}$ denote projected log expenditure for decile h, with the upper and lower tails represented by the top and bottom deciles, respectively. We define the regional support bounds as the 1st and 99th percentiles of observed log expenditure, denoted by xLo_r and xHi_r.

Normalized upper- and lower-tail exceedances are computed using bandwidth $b > 0$:

$$u^H_{r,t} = \text{clip}\left(\frac{m^H_{r,t} - xHi_r}{b}, 0, 1\right), \qquad u^L_{r,t} = \text{clip}\left(\frac{xLo_r - m^L_{r,t}}{b}, 0, 1\right).$$

These exceedances are first transformed into tail-specific transition weights through a smooth monotonic mapping (i.e., $w^H_{r,t} = f(u^H_{r,t})$ and $w^L_{r,t} = f(u^L_{r,t})$), and then combined into a single blending weight:

$$w_{r,t} = \max\left(w^L_{r,t}, w^H_{r,t}\right).$$

The blended shares are then:

$$s^{\text{blend}}_{r,g,h,t} = (1 - w_{r,t})\, s^{\text{Reg}}_{r,g,h,t} + w_{r,t}\, s^{\text{Glob}*}_{r,g,h,t},$$

where $s^{\text{Glob}*}$ denotes the pooled prediction after Stage 2 adjustment.

In the analysis, we set the transition period to five times the width of the historical tail, so that the blending is completed smoothly beyond the observed range. The region-, time-, and scenario-specific blending weights computed and used in the analysis are shown in Fig. S5.

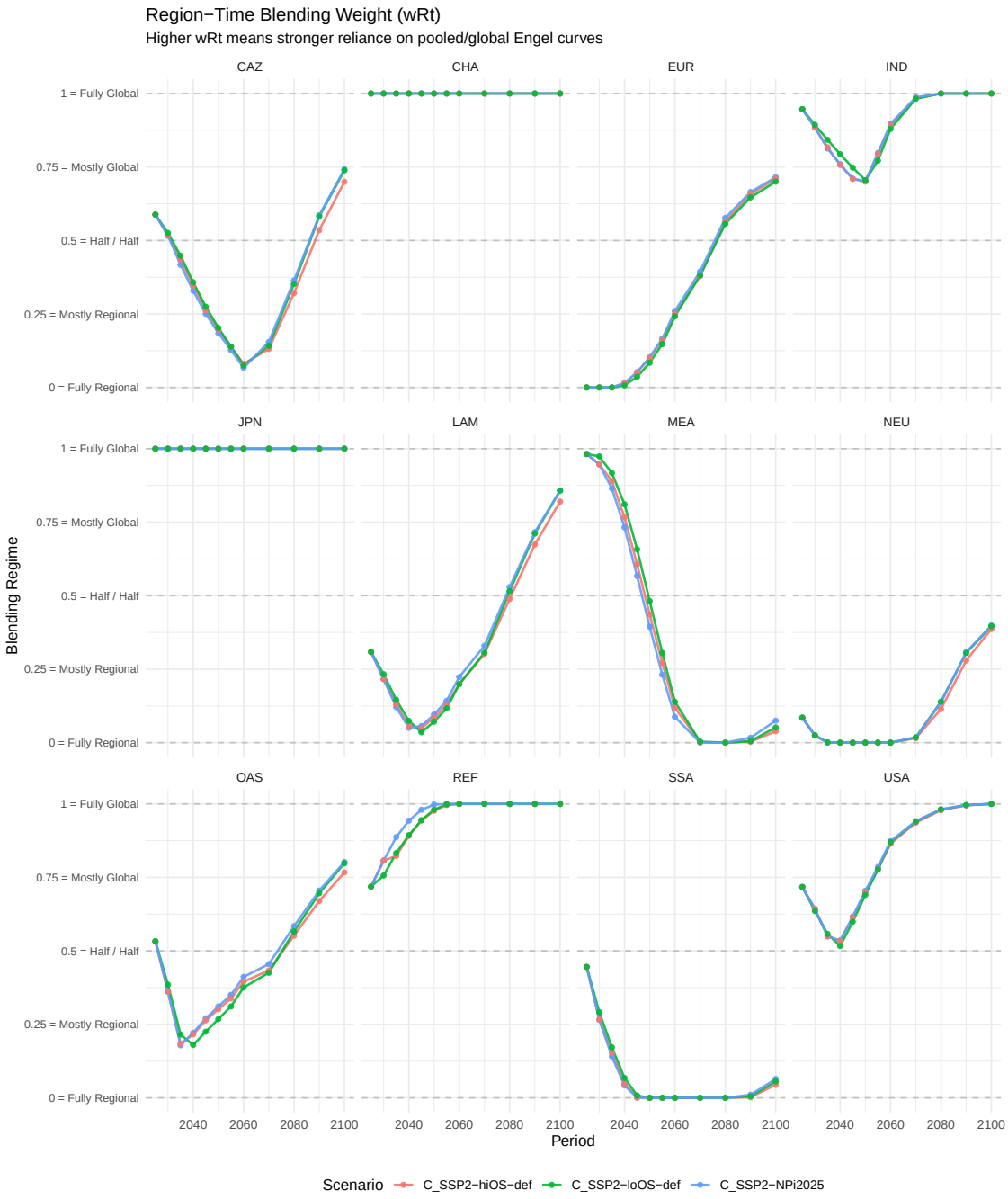

Supplementary Figure S5: Dynamic region–global blending weight. Illustration of the transition weight $w_{r,t}$ that governs the smooth shift from region-specific Engel-curve projections to pooled global projections when projected expenditures move beyond regional empirical support.

Stage 2: Upper-tail shape restriction Stage 2 addresses instability in the upper tail of pooled Engel curves. Although the pooled global curve is estimated over a much wider range of observed expenditures, it still does not fully cover the expenditure levels projected through 2100. We therefore also assess whether extrapolation of the pooled curve leads to unreliable projections.

For a subset of categories, unconstrained quadratic specifications imply excessively steep declines in expenditure shares, leading to implausible reductions in absolute consumption at high expenditure levels.

Because this is an extrapolation issue rather than evidence that absolute consumption in these categories should decline at high expenditure levels, we impose shape restrictions on selected pooled Engel curves. Let x denote total expenditure and $z = \log x$, with pooled latent index:

$$\ell_g(z) = \text{logit}(s_g(x)) = a_g + b_g z + c_g z^2,$$

and slope:

$$\ell'_g(z) = b_g + 2c_g z.$$

Over the upper-tail interval $z \in [z_L^G, z_U^G]$, we impose:

$$-1 \leq \ell'_g(z) \leq 0.$$

The lower bound allows moderate declines in shares, while ruling out implausibly strong negative responses in absolute expenditure. The upper bound prevents continued increases driven by polynomial curvature.

The constraint is activated only beyond the empirical pooled support:

$$z_L^G = \log(Q_{0.99}(x)),$$

and extends to:

$$z_U^G = \log\left(\kappa x_{\max}^{\text{hist}}\right), \qquad \kappa \approx 3.2,$$

The value of κ is data-driven and is set to align the extrapolation range with projected expenditure levels relative to the historical maximum.

The two stages are sequential and complementary. Stage 1 governs the transition from region-specific to pooled behavior once projections leave regional support. Stage 2 disciplines pooled behavior in the extreme upper tail. Together, they ensure stable extrapolation while preserving regional heterogeneity where supported by data.

S4.2 Consistency adjustment via matrix balancing (RAS)

The decile-level consumption shares projected from Engel curves do not, in general, aggregate to the macroeconomic expenditure composition implied by the IAM. This discrepancy arises because

Engel-curve projections are anchored in historical consumption patterns, whereas future consumption structures may evolve with rising expenditures and with demand-side assumptions embedded in the IAM or underlying SSPs. To ensure consistency between micro-level projections and macro-level outcomes, we apply a matrix-balancing procedure based on a weighted RAS (iterative proportional fitting, IPF) algorithm.

For each region r, period t, and scenario, let S_{hg}^{raw} denote the decile-by-good matrix used as the initial input to RAS, with entries given by the blended shares $s_{r,g,h,t}^{\text{blend}}$.

The calibration enforces two constraints:

Decile adding-up constraint For each decile, sectoral shares must sum to one:

$$\sum_{g} S_{hg} = 1 \quad \forall h.$$

Macro consistency constraint The expenditure-weighted average of decile shares must reproduce the macroeconomic sectoral composition:

$$\sum_{h} w_h S_{hg} = m_g \quad \forall g,$$

where m_g denotes the macro-level expenditure share of sector g, and w_h are decile weights proportional to decile consumption levels:

$$w_h = \frac{C_h}{\sum_{h'} C_{h'}}.$$

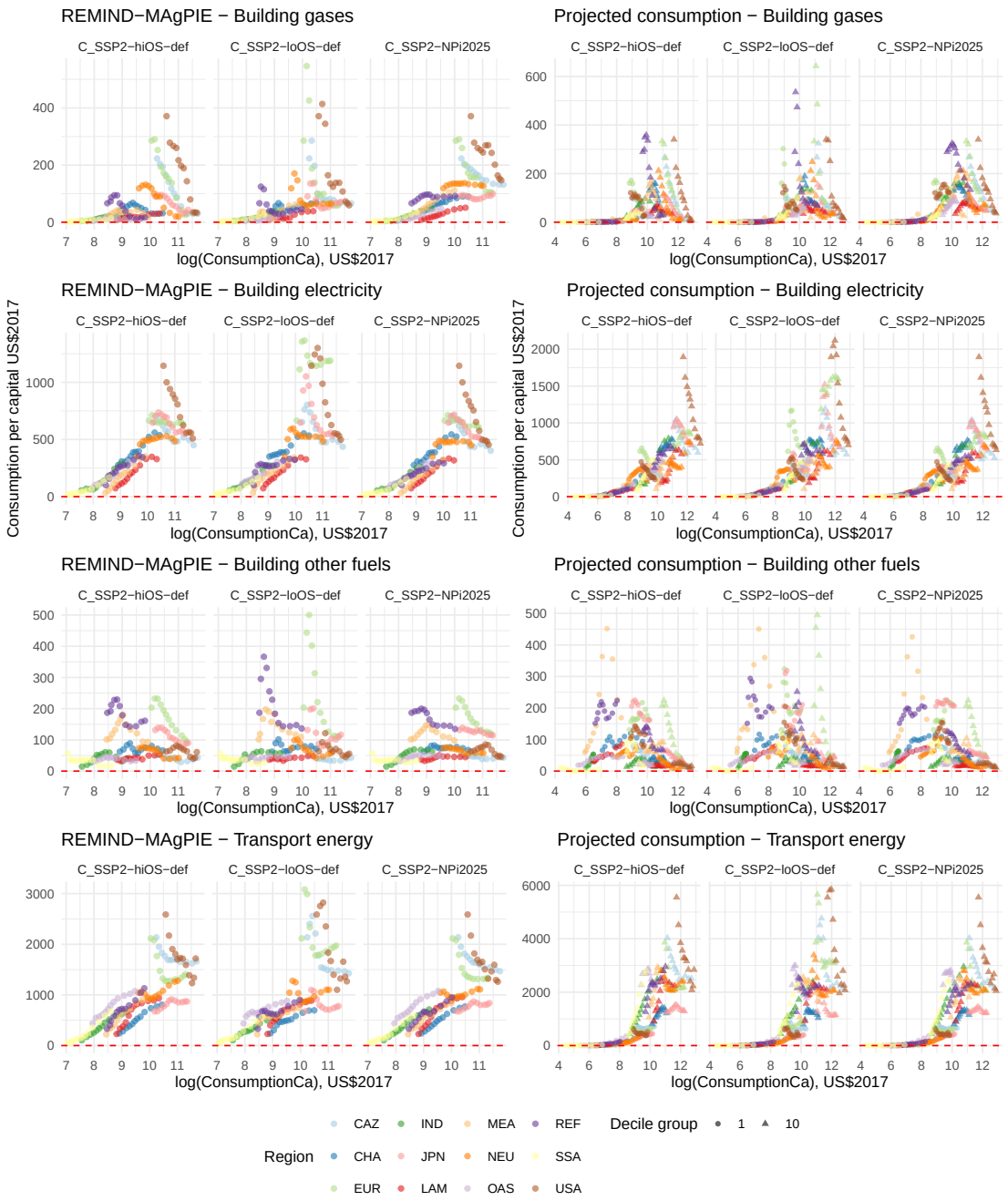

Supplementary Figure S6: Macro-level and projected decile energy consumption.

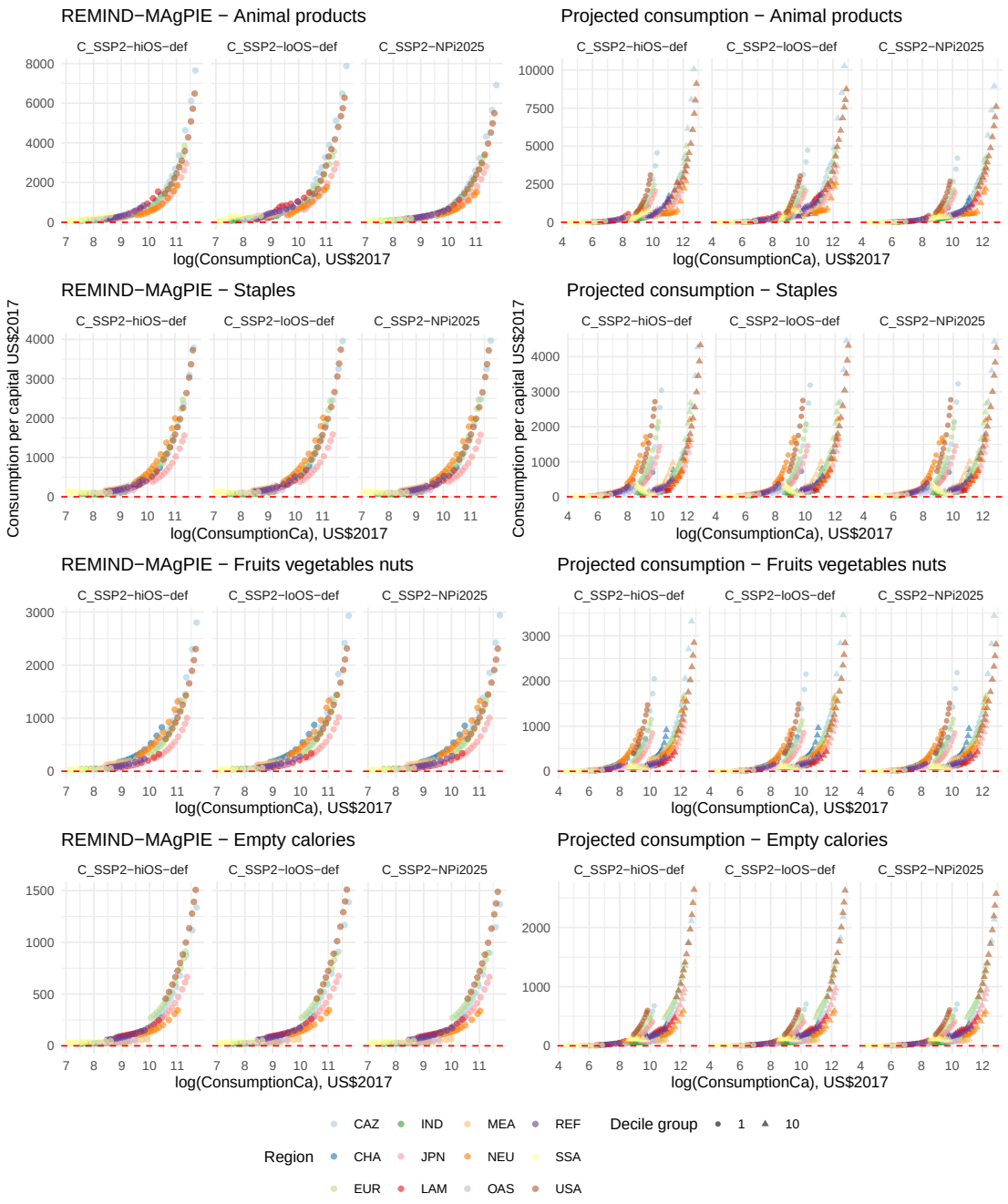

Supplementary Figure S7: Macro-level and projected decile food consumption.

This weighting ensures that the calibrated decile matrix reproduces the macro composition in expenditure terms, giving greater weight to higher-expenditure deciles.

The RAS adjustment preserves the cross-decile structure implied by the Engel curves as much as possible, while enforcing exact consistency with macroeconomic expenditure shares. In this sense, the Engel curves determine the relative distribution of consumption across deciles, and the RAS

step ensures that their aggregation is fully aligned with the IAM-consistent consumption structure.

The final projected absolute consumption values are as follows (see Fig. S6 and Fig. S7)

S5 Financing net negative emissions with global climate fund

In overshoot pathways, net-negative emissions generate negative carbon pricing revenues, reflecting a subsidy requirement for CDR. In cost-efficient IAM pathways, CDR is deployed where it is cheapest, leading to a spatial concentration of net-negative emissions and associated financing requirements. This creates a mismatch between the location of CDR deployment and plausible burden-sharing in real-world settings. Moreover, CDR subsidies may compete with governments' fiscal capacity for social transfers. To maintain fiscal neutrality of the mitigation framework while enabling international burden sharing of CDR costs, we introduce a stylised global climate fund that pools carbon pricing revenues across regions and over time to finance the global net-negative emission requirement.

Operationally, the fund is defined by three rules. First, contribution obligations are assigned only to region–year pairs with positive carbon-pricing revenues, and each contributing region pays a common share τ of its positive revenue in each period; region–year pairs with net-negative CDR receive payouts from the fund. Second, solvency is enforced through a no-borrowing condition on the fund balance, $F_t \geq 0$, so payouts for net-negative emissions are always backed by accumulated resources. Third, the mechanism is closed by a terminal condition at the end of the horizon (year 2100), $F_{2100} = 0$, implying that all CDR-related financing obligations are fully paid within the model horizon and no residual surplus or deficit is carried beyond 2100.

Let $R_{r,t}$ denote regional carbon pricing revenue in region r and period t, with $R^+_{r,t} = \max(R_{r,t}, 0)$ and $R^-_{r,t} = \min(R_{r,t}, 0)$ denoting its positive and negative components, respectively. The global financing requirement associated with net-negative emissions is defined as the non-negative payout requirement

$$P_t = -\sum_r R^-_{r,t}, \qquad P_t \geq 0.$$

Regions with positive carbon revenues contribute a uniform share of revenues to the fund,

$$C_{r,t} = \tau \, R^+_{r,t},$$

where τ is the global contribution rate and contributions are capped by available positive revenues.

Let F_t denote the global fund balance. The fund evolves according to

$$F_{t+1} = (1 + i_t)F_t + \sum_r C_{r,t} - P_t,$$

where i_t is the model-consistent interest rate. The contribution rate τ is chosen such that the fund remains solvent in all periods ($F_t \geq 0$) and closes at the terminal year with $F_{2100} = 0$.

Overall, the global fund separates the location of CDR deployment from its financing by pooling resources across regions and time. Regions with positive carbon revenues contribute to the fund, while the fund covers the global net-negative emission requirement. This ensures a consistent fiscal treatment of CDR within the model and avoids region-specific revenue shortfalls arising from concentrated net-negative emissions.

S6 Distributional Impacts of Climate Policy Costs

S6.1 Consumer price shock

In mitigation scenarios, consumer prices deviate from the NPi baseline due to the introduction of higher carbon pricing and the associated transformation of the energy and production systems. Carbon prices increase the cost of emissions-intensive inputs, particularly fossil fuels and energy services, which are transmitted through production and supply chains to final consumption prices.

Beyond these direct cost effects, structural changes in the energy system, such as the substitution toward low-carbon technologies, shifts in energy carriers, and changes in land use, further alter relative prices across consumption categories. For example, energy prices are affected by both carbon costs and the pace of energy system transition, while food prices reflect interactions between land demand, bioenergy production, and carbon sequestration.

As a result, mitigation pathways generate heterogeneous price changes across consumption categories relative to the NPi2025 baseline, which constitute the primary channel through which climate policy affects household welfare in the distributional analysis.

Below, we show relative price changes in energy and food categories compared with the NPi baseline (Fig. S8). Under the LO scenario, price shocks are strongly front-loaded, peaking around mid-century (≈2045). In contrast, the HO scenario exhibits a more gradual build-up, particularly for food prices, which eventually exceed the peak levels observed under LO.

Across energy categories, a similar pattern emerges. In the LO scenario, price increases are concentrated in the near term and decline after peaking around 2040. By the end of the century, prices for clean energy carriers such as household electricity return to levels close to the NPi baseline,

while fossil-based fuels, including gas and other fuels, remain persistently more expensive due to continued carbon pricing.

In the HO scenario, price increases for cleaner energy carriers are more muted across regions, whereas fossil fuels experience substantially stronger price escalation over time, reaching higher levels by the end of the century. Notably, higher prices do not necessarily translate into large expenditure increases in these categories, because consumption of traditional energy carriers becomes very small during the transition. In the next sections, we examine macro-level category-specific consumption responses.

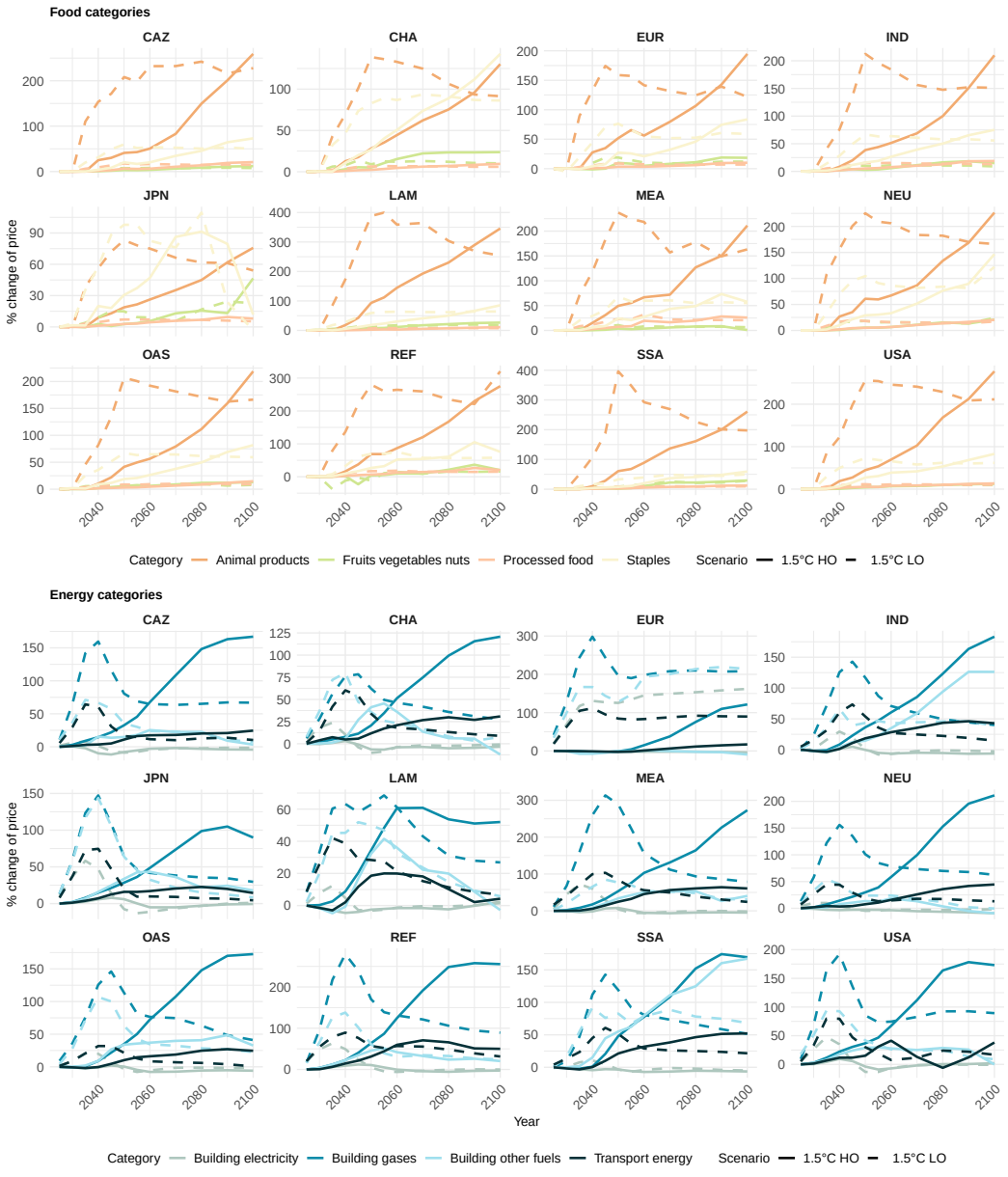

Supplementary Figure S8: Price changes compared to current policy scenario

S6.2 Macroeconomic and regional consumption behavior responses

In the macro framework, mitigation policies affect consumption of different categories mainly through system-level adjustments. In REMIND, carbon pricing raises the cost of emissions-intensive energy carriers and shifts the system toward low-carbon technologies, changing the relative prices of energy categories such as electricity, gaseous fuels, and liquid fuels. In MAgPIE, food categories are affected by changes in agricultural production costs, land allocation, trade, and limited demand responses to price and expenditure. Together, these processes generate category-specific changes in prices and consumption, which are then mapped onto household consumption baskets in the distributional framework to assess welfare impacts.

The regional consumption expenditure dynamics across all eight categories, relative to the NPi baseline, are shown in Fig. S9. A key distinction between food and energy categories is that food expenditure is generally higher in mitigation scenarios than in NPi. As these values reflect expenditure, the increase is primarily driven by higher prices, while food demand remains sufficiently inelastic such that total spending remains stable or increases.

Energy categories show a contrasting pattern. Despite higher prices, total expenditure declines relative to NPi. This reflects a substantial reduction in the use of traditional energy sources, such as gas and solid fuels, which more than offsets the price increases.

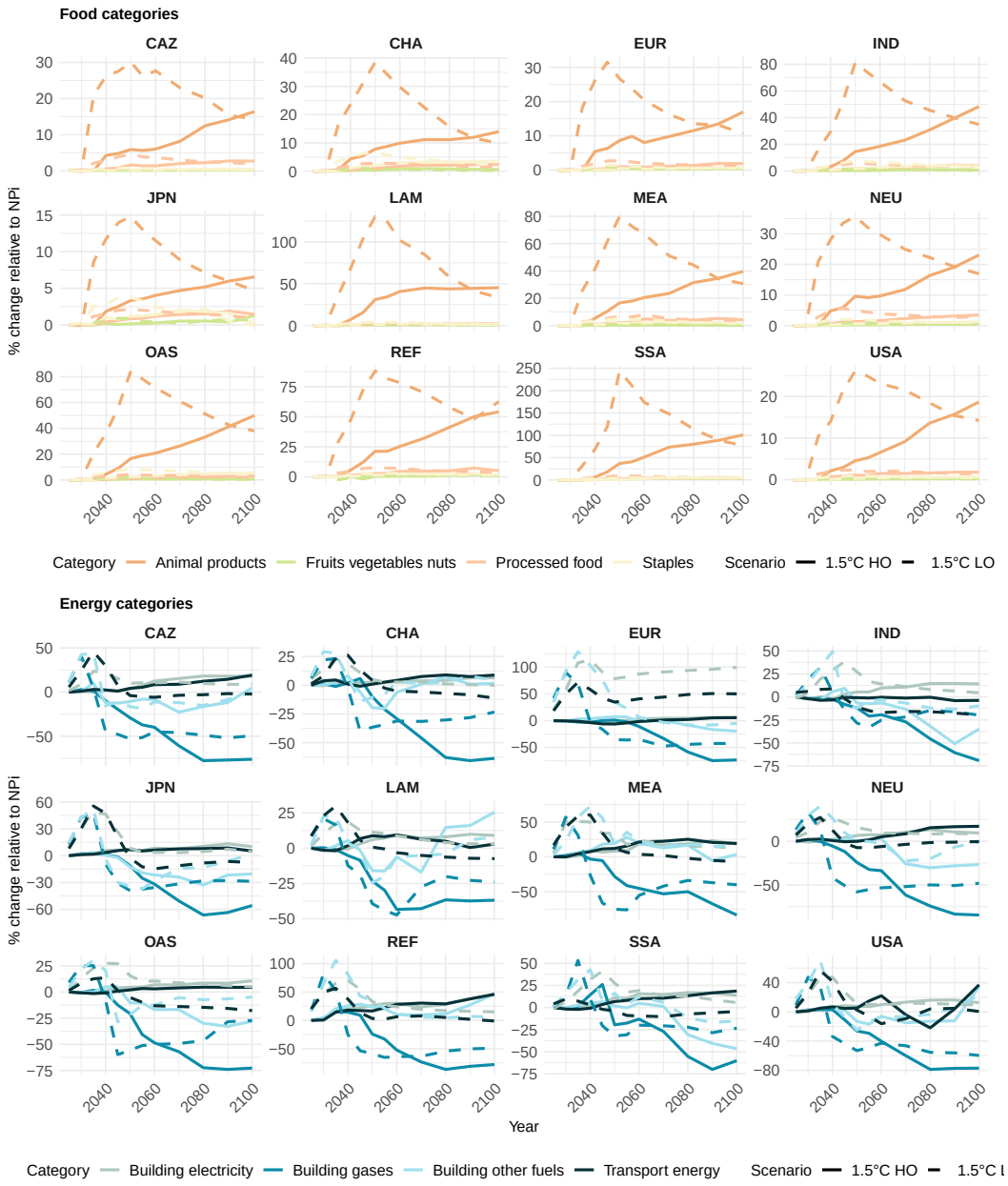

Supplementary Figure S9: Regional consumption expenditure dynamics compared to NPi

S6.3 Sectoral contributions to cost-of-living index (COLI)

Welfare changes induced by consumer price variations are quantified using a cost-of-living index (COLI), which measures the change in expenditure required for households to maintain a given level of utility under evolving prices and consumption patterns. An increase in the COLI therefore reflects a higher cost of maintaining real consumption (a welfare loss), while a decrease indicates a welfare gain.

For region r, decile h, and year t, the change in the COLI is defined as

$$\Delta \ln P_{r,h,t} = \sum_{g} \bar{w}_{g,r,h,t} \left(\ln p'_{g,r,t} - \ln p_{g,r,t} \right), \tag{1}$$

$$\bar{w}_{g,r,h,t} = \tfrac{1}{2} \left(w_{g,r,h,t} + w'_{g,r,h,t} \right), \tag{2}$$

where $\bar{w}_{g,r,h,t}$ denotes the average of baseline and policy expenditure shares.

The Törnqvist index uses the arithmetic mean of expenditure shares as weights. It is exact under translog preferences and provides a second-order approximation more generally, treating baseline and policy states symmetrically and reducing bias when consumption shares adjust in response to price changes.

Differences in COLI across scenarios and expenditure deciles capture the combined effects of price changes, macroeconomic adjustments, and distributional shifts, providing a consistent metric to evaluate heterogeneous welfare impacts of mitigation policies.

Regional, decile-level changes in COLI are reported in Fig. S10 and Fig. S11 for the two scenarios.

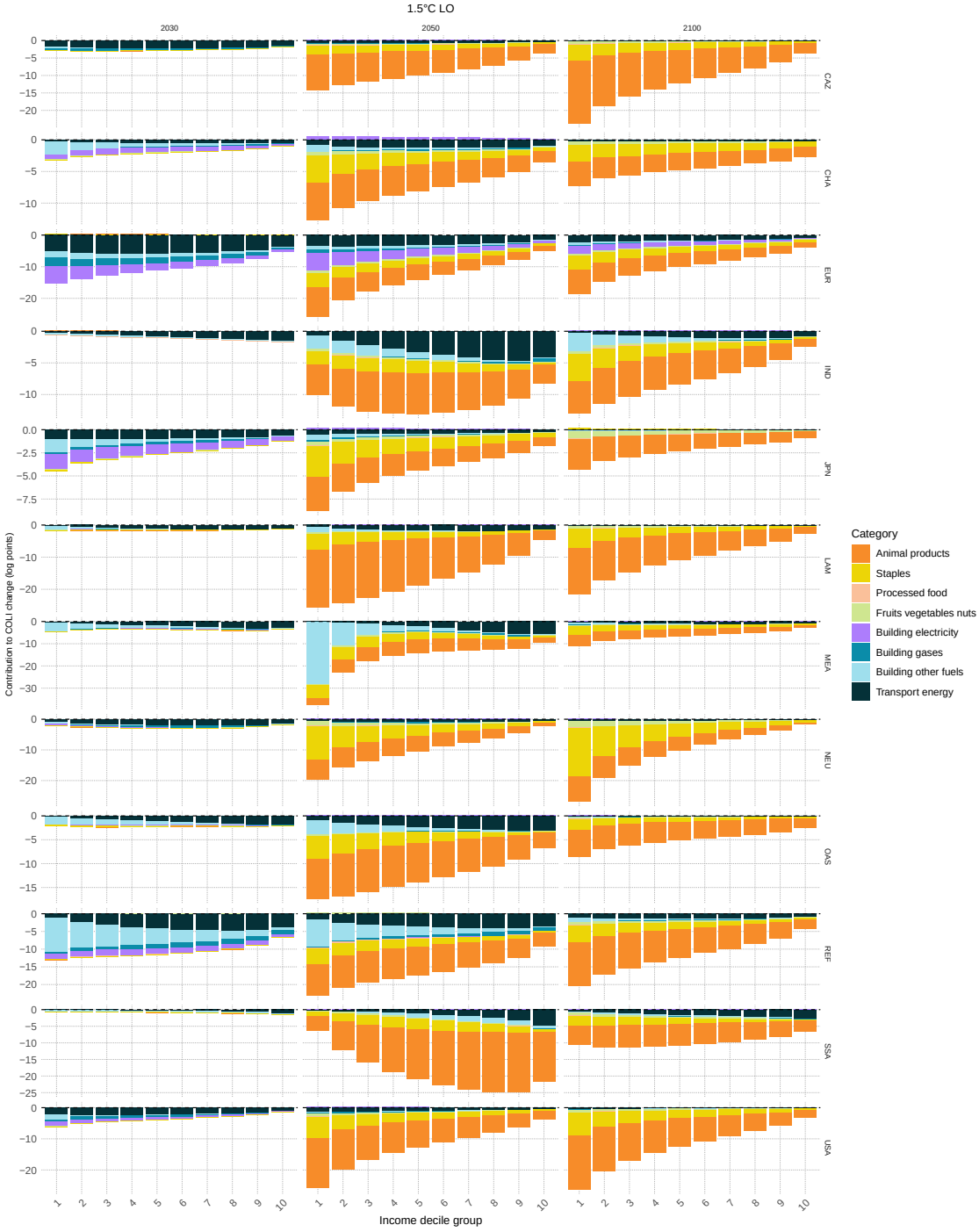

Supplementary Figure S10: Changes in the cost-of-living index across deciles in selected periods under the low-overshoot pathway.

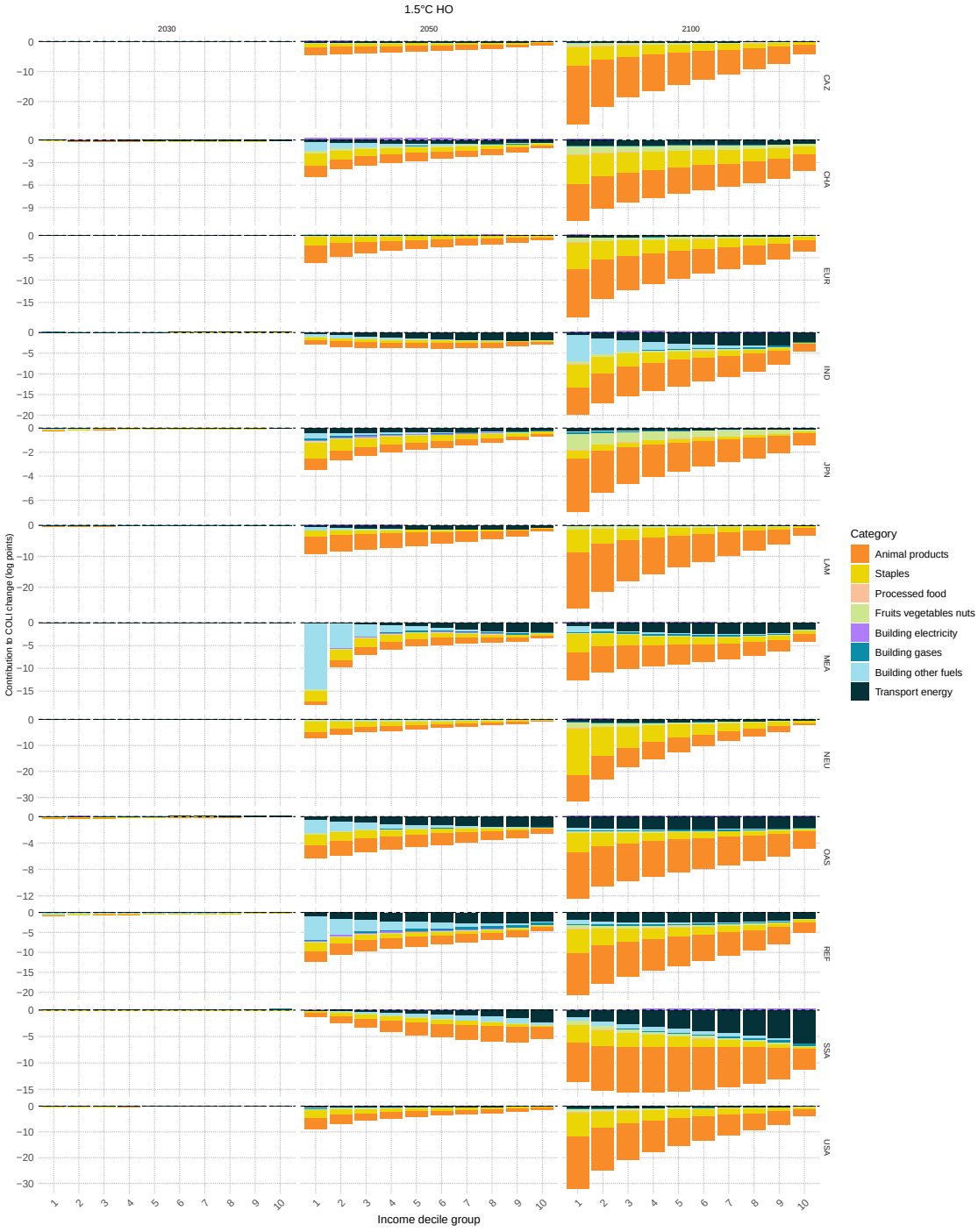

Supplementary Figure S11: Changes in the cost-of-living index across deciles in selected periods under the high-overshoot pathway.

S7 Inequality Metrics and Decomposition

S7.1 Measures of inequality (Gini, Theil)

This subsection defines the inequality indicators used in the main text and supplementary analysis. We report both Gini- and Theil-based measures to ensure that the core findings are not driven by the choice of metric.

The Gini coefficient summarizes inequality based on the Lorenz curve and ranges from 0 (perfect equality) to 1 (maximum inequality), with greatest sensitivity around the middle of the distribution. We also report Theil indices from the generalized entropy class: Theil T is more sensitive to changes at the upper end of the distribution, whereas Theil L (mean log deviation) places more weight on changes at the lower end. All measures are calculated from decile-level consumption distributions by region and time period. The Theil indices also allow additive decomposition, which we use to separate within-region and between-region contributions to overall inequality. Global inequality measured by the Theil index shows a similar trend to the Gini coefficient (Fig. S12).

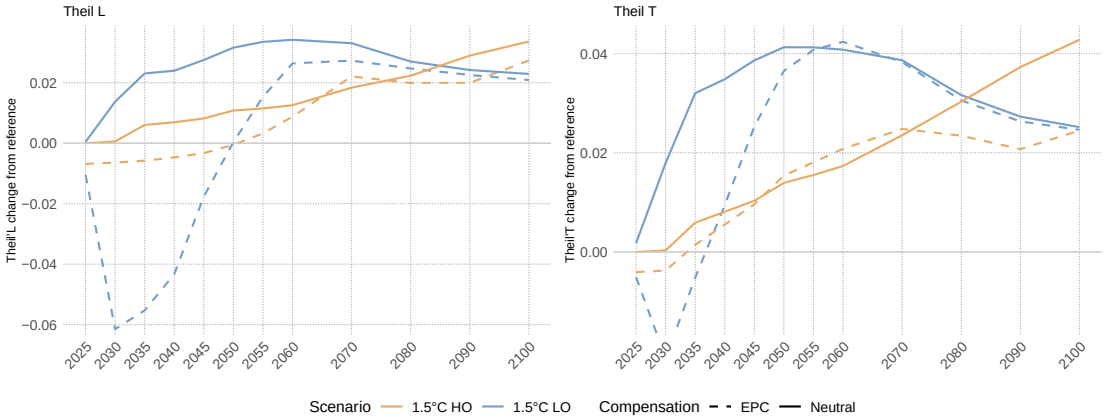

Supplementary Figure S12: Global inequality dynamics measured by the Theil index.

S7.2 Between- and within-country decomposition

We decompose aggregate inequality into between-country and within-country components using the Theil L index. This decomposition clarifies whether pathway differences are primarily associated with cross-country divergence or with distributional changes within regions.

The results show that changes in global inequality are predominantly driven by within-country dynamics across all scenarios and policy designs, while between-country contributions remain comparatively small throughout the century. Under the climate fund and EPC transfer schemes, within-country inequality is reduced in the early decades (up to around 2060), reflecting the availability

of positive carbon revenues and their redistributive use (Fig. S13).

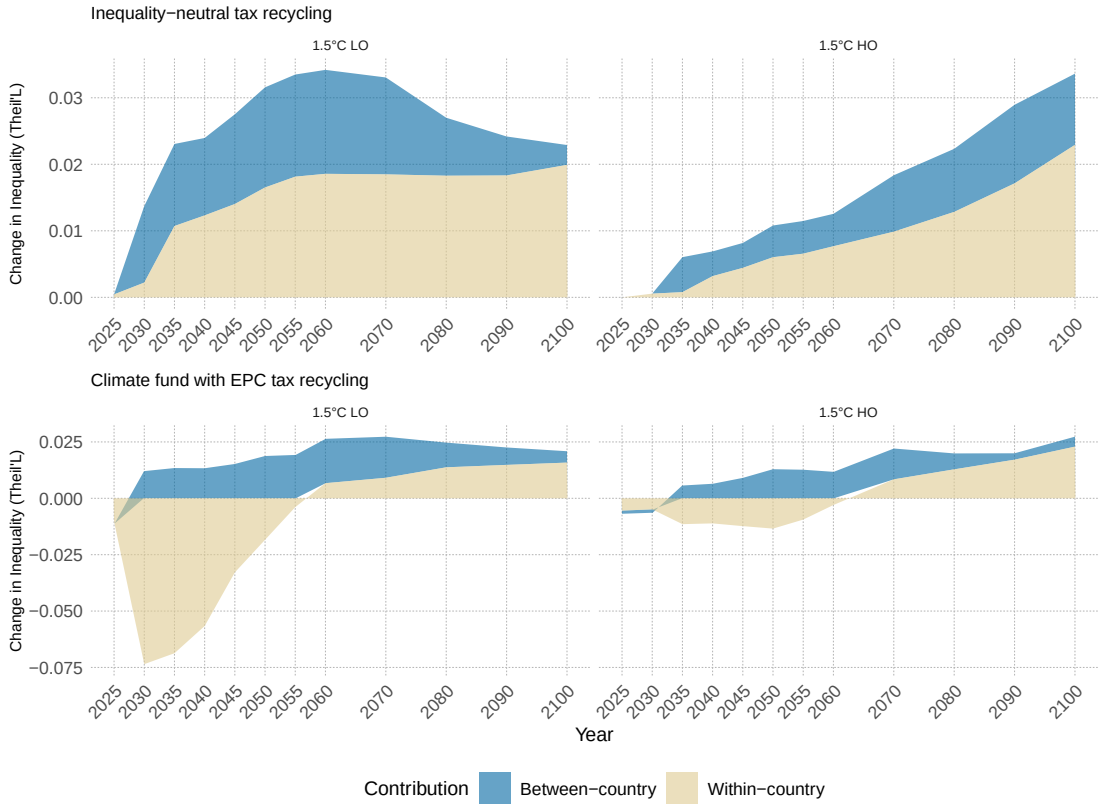

Supplementary Figure S13: Global inequality decomposition under different scenarios and tax-recycling schemes.

S7.3 Shapley decomposition of sectoral contributions

To quantify the contribution of sector-specific price changes to inequality, we apply a Shapley decomposition. A key challenge in this context is that price changes across consumption categories occur simultaneously and interact through household expenditure responses, making simple one-at-a-time or residual-based attributions sensitive to ordering and unable to fully capture interaction effects.

The Shapley approach addresses this by averaging marginal contributions across all possible orderings of category inclusion, yielding a path-independent and internally consistent decomposition. This allows us to attribute the overall change in inequality to individual consumption categories in a way that is robust to cross-sector interactions.

Starting from the baseline consumption distribution under the NPi2025 scenario, we construct decile-specific consumption changes induced by sectoral price shocks. These shocks are scaled such

that, when combined, they reproduce the total price-induced change in real consumption for each decile.

We then evaluate inequality changes as sectoral shocks are introduced sequentially. Each sector is treated as a "player" contributing to the overall inequality change. Beginning from the baseline distribution, sectoral shocks are added one at a time, and the resulting change in the inequality index is recorded after each addition. Because the marginal contribution of a given sector depends on the order of inclusion, we repeat this procedure across all possible orderings (or a large set of random permutations) and compute the average marginal contribution of each sector.

The resulting Shapley values provide an order-independent decomposition of the total change in inequality into sector-specific contributions. This ensures that interaction effects between sectors are fully accounted for and that contributions sum exactly to the total inequality change. The decomposition is applied separately for each scenario, region, period, and inequality measure (Gini, Theil-L, and Theil-T).

S8 Broader Tax Base for Government Revenue

S8.1 Carbon pricing and definition of tax revenues

In the macro framework, climate policy is represented by a region-time specific carbon price that emerges endogenously as the shadow price of the emissions constraint. This price therefore reflects the marginal abatement cost required to meet a given temperature target, rather than a fiscal instrument explicitly levied by governments. Consequently, the associated "tax revenues" are not modeled directly as government income and require additional interpretation in the distributional analysis.

To construct a measure of feasible government revenue, we interpret the carbon price as a proxy for real-world carbon pricing instruments and apply it to selected emission sources. Our main specification focuses on GHG emissions from the energy system, which constitute the most plausible tax base because existing carbon pricing schemes are implemented predominantly in this domain. This approach provides a conservative and policy-relevant estimate of carbon-related fiscal capacity.

By contrast, extending the tax base to agricultural non-CO_2 emissions, such as CH_4 and N_2O, is technically feasible within the model but remains institutionally and politically challenging in practice. Measurement difficulties, diffuse emission sources, and concerns about impacts on food systems have limited the adoption of such pricing in real-world policy. We therefore include agricultural emissions only in supplementary analyses to illustrate the sensitivity of the results to broader tax bases.

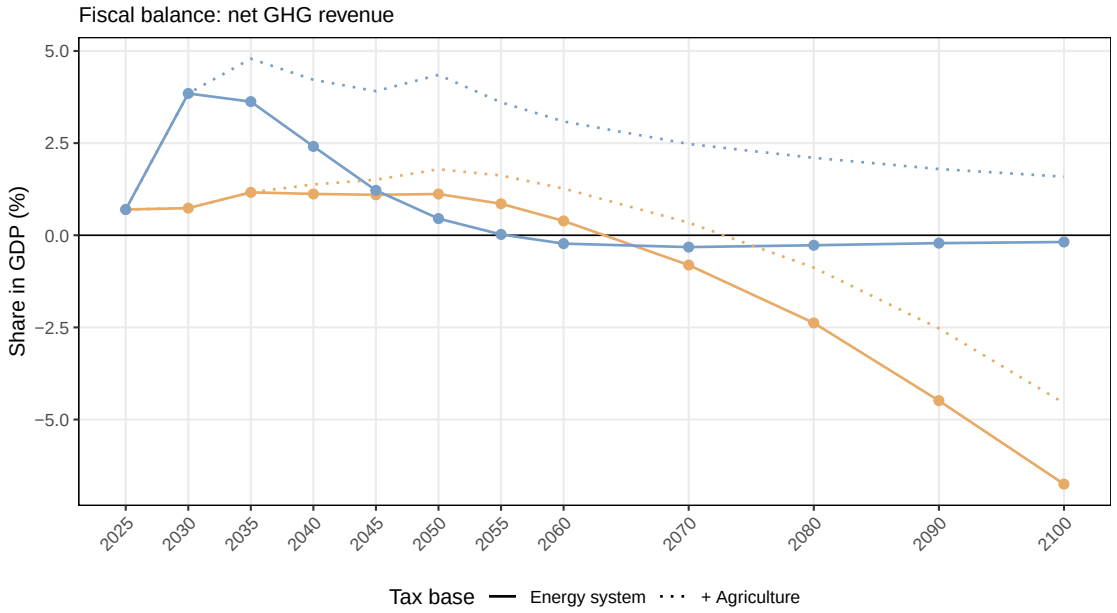

Supplementary Figure S14: Government revenue potential under alternative carbon tax bases

Including agricultural emissions improves mitigation-related fiscal balance (Fig. S14). Because some agricultural emissions are difficult to abate, they continue to generate revenue after the energy system reaches net carbon zero. As a result, they create an additional positive revenue stream in the LO pathway and substantially alleviate fiscal stress in the HO pathway.

An even more ambiguous case concerns emissions and removals from land-use change (LUC), including afforestation and reforestation. While these fluxes are fully represented in the coupled REMIND – MAgPIE framework and are subject to the model' s carbon price, their interpretation as a taxable base is less straightforward. First, LUC-related carbon fluxes are subject to substantial measurement uncertainty and depend on baseline definitions (e.g., additionality and counterfactual land use), complicating their use in a fiscal context. Second, a large share of these activities is incentivized through subsidies or crediting mechanisms rather than taxed in practice, implying fundamentally different policy instruments. Third, LUC mitigation is often implemented through land management policies, conservation programs, or carbon markets with heterogeneous accounting rules, rather than uniform taxation.

For these reasons, including LUC-related emissions and removals in the tax base would blur the distinction between carbon pricing as a revenue-generating instrument and broader climate policy support schemes. We therefore exclude LUC components from the main analysis to maintain a transparent and policy-relevant definition of fiscal capacity.

S8.2 Distributional analysis with broader carbon tax base

Here, we simulate the global climate fund and regional EPC redistribution under the broader carbon tax base. The global climate fund required to finance CDR becomes much smaller because the broader tax base reduces the need for such financing (Fig. S15). Under the low-overshoot pathway, there is no net-negative CDR and therefore no need for a climate fund. Under the high-overshoot pathway, financing for net-negative CDR is still required, but the fund size is much smaller: the uniform saving rate falls to 0.242, substantially below the level in the case where only energy-system emissions are taxed.

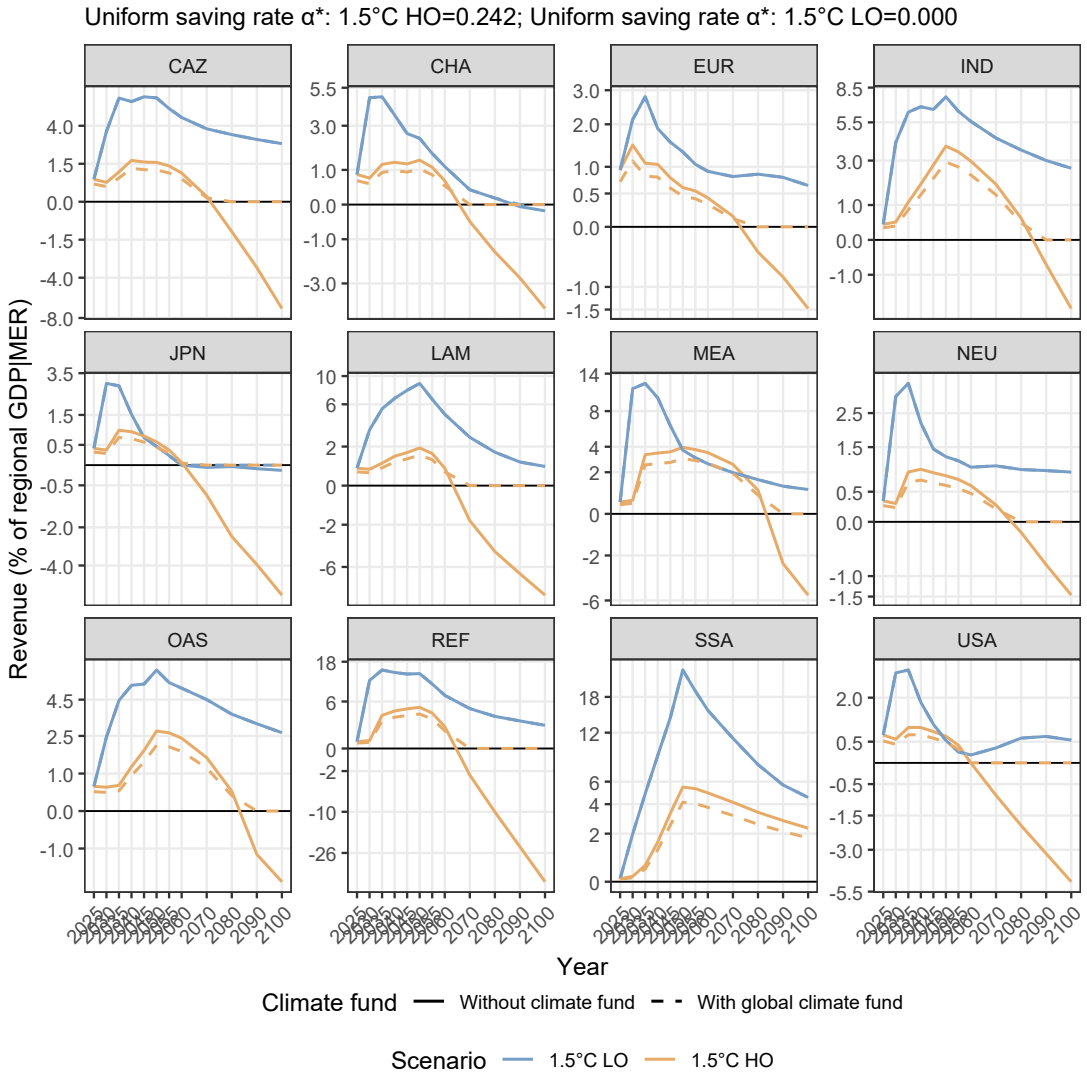

Supplementary Figure S15: Regional net mitigation revenue flows with and without the Global Climate Fund

With a broader tax base, governments can achieve better distributional outcomes at both the global and regional levels through the Climate Fund and EPC transfers across all periods (Fig. S16). This suggests that taxing agricultural emissions could potentially provide ample fiscal resources to address distributional concerns. At the same time, such an approach remains difficult to implement in practice and may not be distribution-neutral, because it could also affect farmers through the income channel, which we are not able to assess in this analysis.

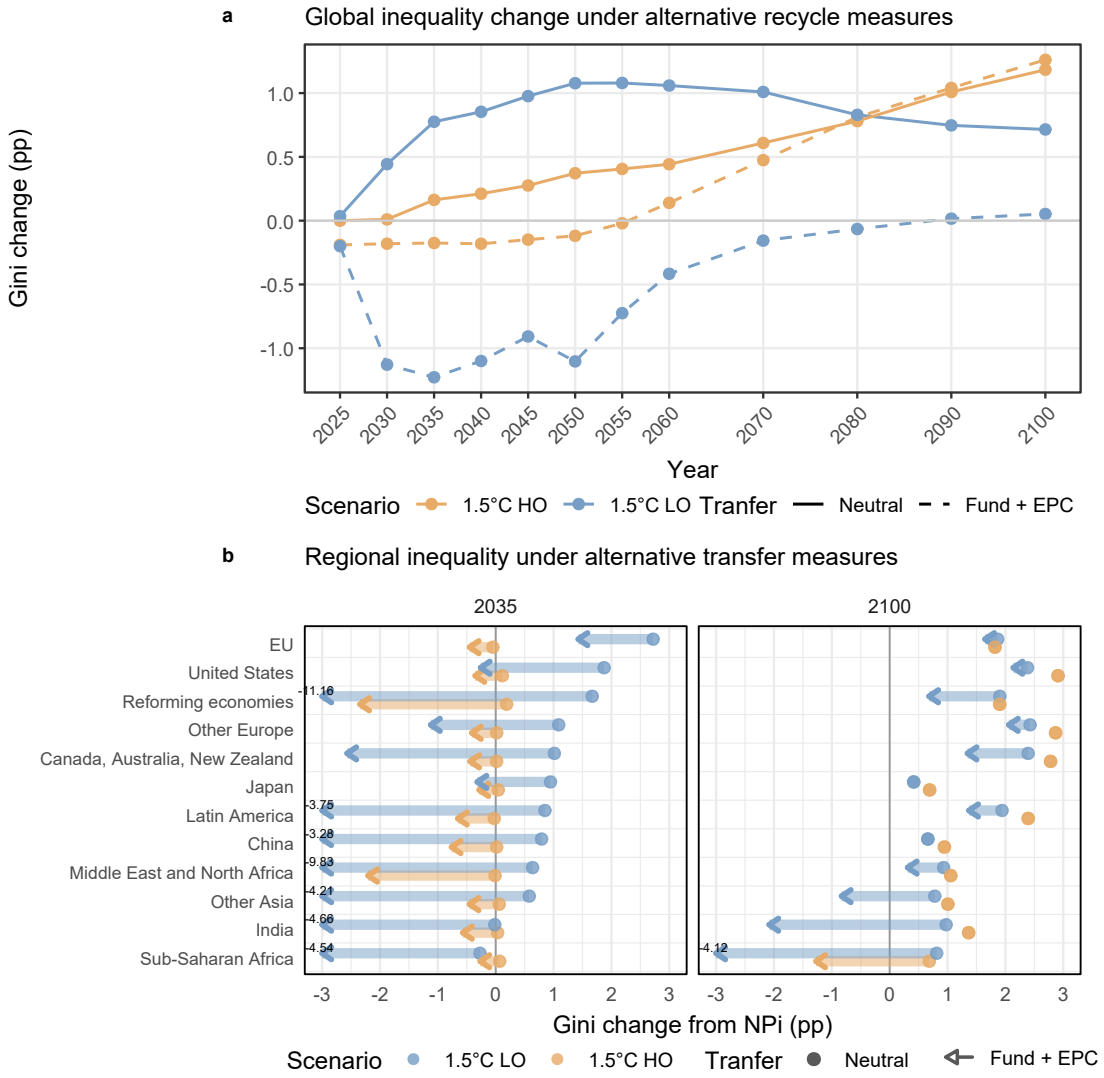

Supplementary Figure S16: Global and regional inequality under progressive redistribution with a broader tax base

References

[1] Narasimha D. Rao, Petra Sauer, Matthew Gidden, and Keywan Riahi. Income inequality projections for the Shared Socioeconomic Pathways (SSPs). *Futures*, 105:27–39, January 2019. ISSN 0016-3287. doi: 10.1016/j.futures.2018.07.001.

[2] Keywan Riahi, Detlef P. van Vuuren, Elmar Kriegler, Jae Edmonds, Brian C. O'Neill, Shinichiro Fujimori, Nico Bauer, Katherine Calvin, Rob Dellink, Oliver Fricko, Wolfgang Lutz, Alexander Popp, Jesus Crespo Cuaresma, Samir Kc, Marian Leimbach, Leiwen Jiang, Tom Kram, Shilpa Rao, Johannes Emmerling, Kristie Ebi, Tomoko Hasegawa, Petr Havlik, Florian Humpenöder, Lara Aleluia Da Silva, Steve Smith, Elke Stehfest, Valentina Bosetti, Jiyong Eom, David Gernaat, Toshihiko Masui, Joeri Rogelj, Jessica Strefler, Laurent Drouet, Volker Krey, Gunnar Luderer, Mathijs Harmsen, Kiyoshi Takahashi, Lavinia Baumstark, Jonathan C. Doelman, Mikiko Kainuma, Zbigniew Klimont, Giacomo Marangoni, Hermann Lotze-Campen, Michael Obersteiner, Andrzej Tabeau, and Massimo Tavoni. The Shared Socioeconomic Pathways and their energy, land use, and greenhouse gas emissions implications: An overview. *Global Environmental Change*, 42:153–168, 2017. ISSN 09593780. doi: 10.1016/j.gloenvcha.2016.05.009.

[3] S. K. C., M. Dhakad, M. Potančoková, S. Adhikari, D. Yildiz, M. Mamolo, T. Sobotka, K. Zeman, G. Abel, W. Lutz, and A. Goujon. Updating the Shared Socioeconomic Pathways (SSPs) Global Population and Human Capital Projections. February 2024.

[4] Bjoern Soergel, Elmar Kriegler, Benjamin Leon Bodirsky, Nico Bauer, Marian Leimbach, and Alexander Popp. Combining ambitious climate policies with efforts to eradicate poverty. *Nature Communications*, 12(1):2342, April 2021. ISSN 2041-1723. doi: 10.1038/s41467-021-22315-9.

[5] Stephen P. Jenkins. World income inequality databases: An assessment of WIID and SWIID. *The Journal of Economic Inequality*, 13(4):629–671, December 2015. ISSN 1569-1721, 1573-8701. doi: 10.1007/s10888-015-9305-3.

[6] Petra Sauer, Narasimha D. Rao, and Shonali Pachauri. Explaining Income Inequality Trends: An Integrated Approach. In Sanghamitra Bandyopadhyay and Juan Gabriel Rodríguez, editors, *Mobility and Inequality Trends*, volume 30, page 0. Emerald Publishing Limited, January 2023. ISBN 978-1-80382-902-9. doi: 10.1108/S1049-258520230000030001.

[7] Leonard Missbach and Jan Steckel. Compensation Design for Carbon Pricing with Horizontal Heterogeneity: Evidence from 88 Countries, 2025.